Journal of Organometallic Chemistry 891 (2019) 44–53

Contents lists available at ScienceDirect

Journal of Organometallic Chemistry

journal homepage: www.elsevier.com/locate/jorganchem

Synthesis and structural characterisation of 1'-(diphenylphosphino) ferrocene-1-phosphonic acid, its ammonium salts and Pd(II) complexes

Filip Horký, Ivana Císařová, Jiří Schulz, Petr Štěpnička*

Department of Inorganic Chemistry, Faculty of Science, Charles University, Hlavova 2030, 12840, Prague, Czech Republic

ARTICLE INFO

Article history:
Received 1 March 2019
Received in revised form
28 March 2019
Accepted 11 April 2019
Available online 17 April 2019

Keywords:
Ferrocene
Phosphine ligands
Phosphonates
Palladium complexes
Structure elucidation
DFT computations

ABSTRACT

A new polar phosphinoferrocene ligand, viz. 1'-(diphenylphosphino)ferrocene-1-phosphonic acid (H_2**L**), was prepared by hydrolysis of the corresponding phosphonate ethyl ester. However, the compound is relatively unstable, gradually decomposing upon prolonged storage, ultimately affording phosphine oxide H_2**L**O. When the phosphine moiety was protected (*e.g.*, in phosphine oxide H_2**L**O and adduct H_2**L**·BH_3), no decomposition was observed. An alternative approach to prepare more stable H_2**L** surrogates by converting the phosphonic acid into ammonium salts (dabcoH)(H**L**) and [$(OHCH_2CH_2)_2NH_2$](H**L**) (dabco = 1,4-diazabicyclo[2.2.2]octane) resulted in no significant stabilisation. H_2**L** reacted with [$PdCl_2$(cod)] (cod = cycloocta-1,5-diene), producing the bis(phosphine) complex, *trans*-[$PdCl_2$(H_2**L**-κ*P*)$_2$]. When mixed with Pd(II)-acetylacetonate (acac) complexes with *ortho*-metallated auxiliary ligands, [(L^{CY})Pd(acac)] (L^{CY} = 2-[(dimethylamino-κ*N*)methyl]phenyl-κC^1 and 2-[(methylthio-κ*S*)methyl]phenyl-κC^1), H_2**L** gave rise to bis-chelate complexes of the [(L^{CY})Pd(H**L**-κ^2*O*,*P*)] type. H_2**L**, the ammonium salts featuring the H**L**$^-$ anion, and all Pd(II) complexes were structurally characterised by single-crystal X-ray diffraction analysis. Variations in phosphonate P-O bond lengths observed in the crystal structures were rationalised by DFT computations.

1. Introduction

Introducing polar moieties into phosphine molecules is a time-tested and efficient approach for the design of new hydrophilic ligands [1]. In this regard, acidic functional groups such as carboxylate, phosphonate and especially sulfonate are among the most frequently used polar moieties. Their incorporation into phosphine molecules results in structurally versatile hybrid phosphine ligands with diverse coordination modes and pH-dependent behaviour [2]. However, this approach has been used less often in the chemistry of otherwise ubiquitous phosphinoferrocene ligands [3]. Examples of functional ferrocene phosphines structurally analogous to the widely studied 1,1′-bis(diphenylphosphino) ferrocene (dppf, Scheme 1) [4], include 1'-(diphenylphosphino)-1-ferrocenecarboxylic acid (Hdpf) [5] and the recently reported phosphinoferrocene sulfonate **A** [6] (Scheme 1). The analogous 1-(diphenylphosphino)-1-ferrocenephosphonic acid (H_2**L**) has not yet been reported, although diethyl 1'-(diphenylphosphino)-1-ferrocenephosphonate, the obvious precursor of H_2**L**, has already been prepared, used as a synthetic intermediate [7] and studied as a ligand in Group 12 metal complexes [8]. To expand the series of dppf-like phosphinoferrocene ligands featuring polar acidic functional groups, we prepared H_2**L**, an organometallic analogue of the triphenylphosphine derivative **B** (Scheme 1) [9]. The synthesis and characterisation of H_2**L**, its ammonium salts and palladium(II) complexes are reported in this paper.

2. Results and discussion

2.1. Synthesis and characterisation of H_2**L**, its derivatives and salts

Acid H_2**L** was obtained from a reaction of phosphonate ester **2** [8] with Me_3SiBr followed by hydrolysis [10] (Scheme 2). Even when carefully purified, the acid gradually decomposed at room temperature and at 4 °C. Decomposition is first manifested as sample darkening and broadening of ^{1}H NMR signals. Later, the ^{31}P NMR spectra show resonances due to the corresponding phosphine oxide (δ_P 16.5 and 31.7 in dmso-d_6). Partly decomposed samples of

* Corresponding author.
E-mail address: petr.stepnicka@natur.cuni.cz (P. Štěpnička).

https://doi.org/10.1016/j.jorganchem.2019.04.012
0022-328X/

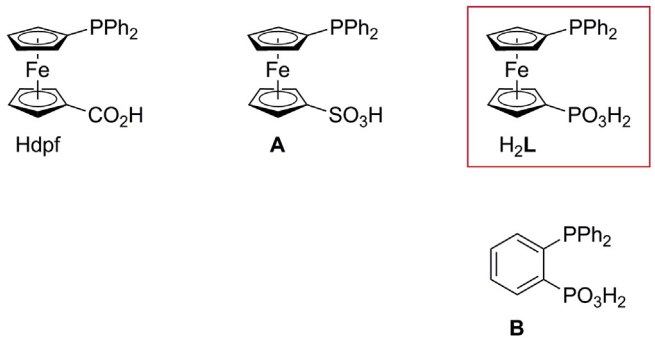

Scheme 1. Polar phosphines relevant to this study.

H_2**L** could be purified by column chromatography (silica gel, chloroform-methanol 10:1), which removed a faster eluting brown band containing unknown decomposition products, followed by an orange band due to H_2**L** and, finally, a slowly moving band containing phosphine oxide H_2**L**O. H_2**L** was also crystallised from ethyl acetate. However, this crystallisation was associated with a substantial loss of crude material and produced easily decomposing, orange crystals.

Attempts to stabilise the phosphino-phosphonate by converting it into crystalline ammonium salts were only partly successful. H_2**L** neutralisation with 1 or 2.5 equiv. of 1,4-diazabicyclo[2.2.2]octane (dabco) and diethanolamine (*i.e.*, 2,2′-iminodiethanol) uniformly led to salts containing the singly deprotonated anion H**L**$^-$, (dabcoH)(H**L**) (**5**) and ((OHCH$_2$CH$_2$)$_2$NH$_2$)(H**L**) (**6**), respectively. Only such salts were obtained, irrespective of the amount of base added, in line with the large differences between the first and second dissociation constants of phosphonic acids (*cf.* pK_{a1} 2.3, pK_{a2} 7.6 for PhCH$_2$PO$_3$H$_2$ [11]). Salts **5** and **6** were spectroscopically and crystallographically characterised, but they nevertheless decomposed upon prolonged storage.

Notably, spontaneous decomposition of ferrocenephosphonic acids, such as FcCH$_2$PO$_3$H$_2$, most likely a self-catalysed oxidation, has already been reported [12]. However, the spontaneous decomposition of the phosphine-substituted derivative H_2**L** may be further complicated by processes involving the phosphine moiety in which the primary decomposition products are converted into the phosphine oxide H_2**L**O. To confirm this assumption, the phosphine oxide H_2**L**O and the phosphine-borane adduct H_2**L**·BH$_3$ were prepared via H_2O_2-oxidation of H_2**L** and analogously to H_2**L** from the P-protected precursor **3**, respectively (Scheme 2). Both H_2**L**O and H_2**L**·BH$_3$ showed no signs of decomposition when stored at room temperature for weeks.

In the ^{1}H NMR spectra, H_2**L** and its P-modified derivatives display four signals due to chemically non-equivalent ferrocene CH groups. These signals broaden into unresolved signals in the spectra of H_2**L** and H_2**L**O, which also show multiplets due to the PPh$_2$ moieties. The presence of the phosphonate moiety is manifested as ^{31}P NMR resonances at $\delta_P \approx 17$ ppm (in dmso-d$_6$). The signal of the phosphine moiety in H_2**L** is observed at δ_P −17.4, whereas this signal appears characteristically shifted to lower field in H_2**L**O and H_2**L**·BH$_3$ (δ_P 31.7 and 15.6 ppm, respectively). H_2**L**, its phosphine oxide, and the borane adduct display the corresponding pseudomolecular ions ([M + H]$^+$) in their ESI mass spectra.

The molecular structure of H_2**L** is depicted in Fig. 1. The compound crystallises unsolvated, with the symmetry of the monoclinic space group $P2_1/n$ and with one formula unit in the asymmetric unit. The individual molecules in the crystal structure assemble *via* O-H···O hydrogen bonds, forming one-dimensional chains along the crystallographic *b* axis (Fig. 2).

Parameters describing the molecular geometry of H_2**L** match those of the respective monofunctional ferrocene derivatives,

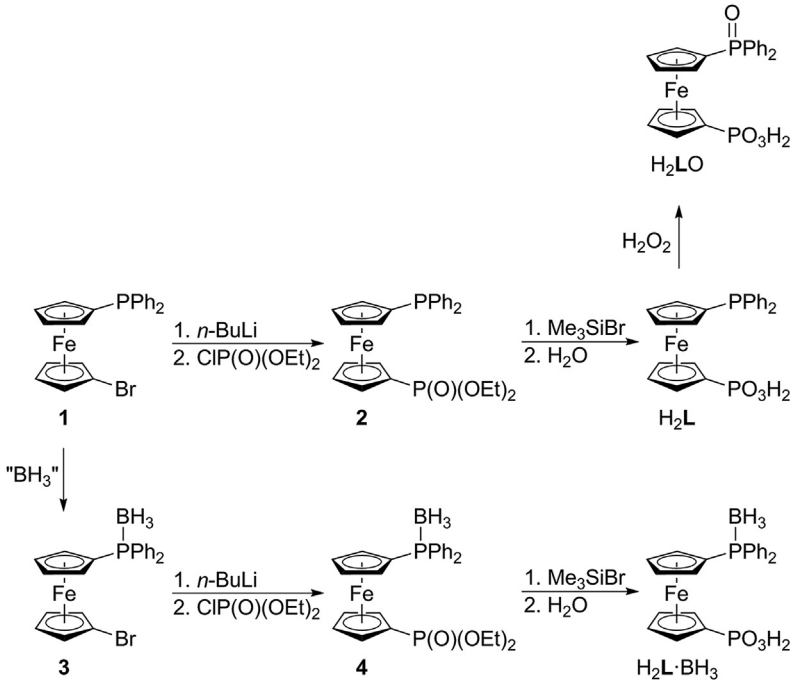

Scheme 2. Synthesis of H_2**L**, its borane adduct H_2**L**·BH$_3$ and phosphine oxide H_2**L**O.

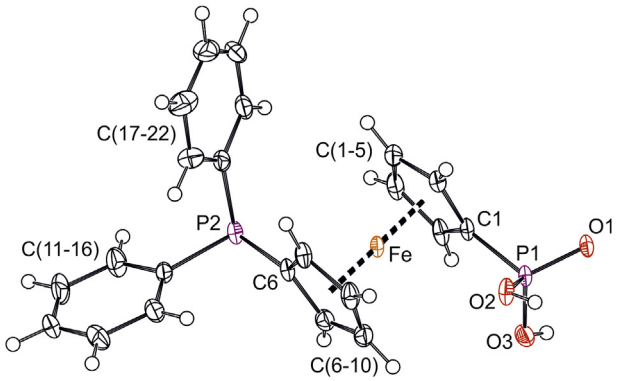

Fig. 1. PLATON plot of the molecular structure of H_2**L** showing atom labelling and displacement ellipsoids at the 50% probability level.

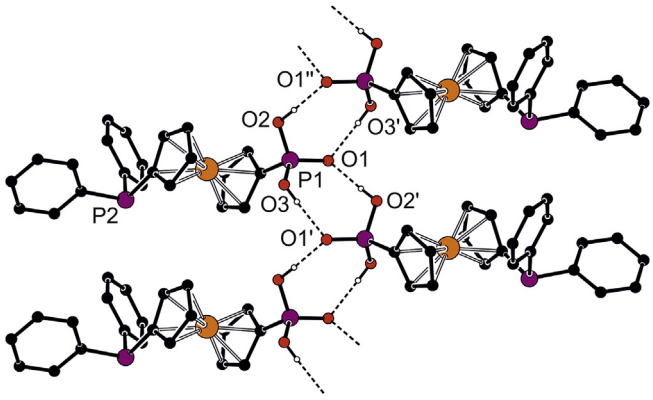

Fig. 2. Section of the hydrogen-bonded assembly in the structure of H_2**L**; for clarity, only OH hydrogens are shown. H-bond parameters: O2···O1 = 2.572(2) Å, O3···O1 = 2.630(2) Å.

$FcPO_3H_2$ [13] and $FcPPh_2$ [14] (Fc = ferrocenyl). The cyclopentadienyl rings in the H_2**L** molecule are essentially parallel (tilt angle: 0.8(1)°), indicating only minor variations in individual Fe-C distances (2.033(2)-2.062(2) Å), and adopt an intermediate conformation between anticlinal eclipsed and antiperiplanar staggered [4b] that brings the substituents to approximately opposite (*anti*) positions, as shown by the τ angle (−165.7(1)°; N.B. τ is the dihedral angle C1-Cg1-Cg2-C6, where Cg1 and Cg2 are the centroids of the cyclopentadienyl rings C(1-5) and C(6-10), respectively).

In addition to free H_2**L**, the crystal structures of salts **5** and **6** were also solved. The molecular structures of the salts are depicted in Fig. 3, and the selected geometric parameters are outlined in Table 1. The ferrocene moieties in the structures of **5** and **6** adopt their regular geometries, showing only insignificant tilting (2.8(2)° in **5**, and 2.9(1)° in **6**). However, they have different conformations. While the ferrocene substituents in **5** adopt rather distant positions, those in **6** are rotated closer to each other (*cf.* the τ angles in Table 1). Notably, the deprotonation of the phosphonate groups markedly differentiates the P-O bonds, presumably due to charge delocalisation. In both salts, the bonds formally attributable to P=O and P-O$^-$ units (P1-O1 and P1-O2) are substantially shorter than the bonds towards the OH groups (P1-O3). On the contrary, the P-O bond lengths of the free acid H_2**L** suggest the presence of one P=O (1.51 Å) and two P-O bonds (1.55 Å). Similar features can be observed when converting phenylphosphonic acid [15] into ammonium salts of the $(R_2NH_2)(PhPO_3H)$ type [16]. In addition,

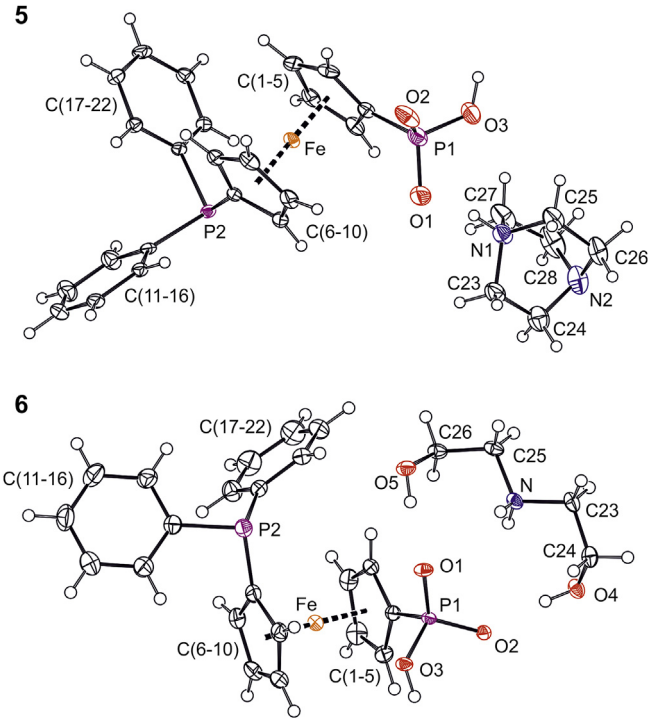

Fig. 3. PLATON plots of the molecules structures of **5** (top) and **6** (bottom); displacement ellipsoids correspond to the 50% probability level.

Table 1
Selected distances and angles for H_2**L**, **5** and **6** (in Å and deg).

Parameter	H_2L	5[a]	6[b]
P-O1	1.510(1)	1.505(3)	1.498(1)
P-O2	1.550(1)	1.509(2)	1.519(1)
P-O3	1.554(2)	1.578(3)	1.577(1)
O1-P1-O2	111.35(7)	116.4(2)	115.48(6)
O1-P1-O3	111.30(8)	106.5(2)	108.53(6)
O2-P1-O3	108.08(8)	111.5(1)	109.01(6)
P1-C1	1.753(2)	1.800(3)	1.787(1)
P2-C6	1.818(2)	1.810(3)	1.820(2)
P2-C11	1.832(2)	1.837(3)	1.839(2)
P2-C17	1.840(2)	1.840(3)	1.835(2)
τ	−165.7(1)	−139.6(2)	85.4(1)

[a] Further data: N-C distance range in $(dabcoH)^+$ = 1.457(6)-1.499(5) Å.
[b] Further data: N-C23 1.492(2), N-C25 1.496(2), O4-C24 1.429(2), O5-C26 1.417(2), C23-N-C25 113.8(1).

deprotonation of the phosphonate moiety results in a shortening of the pivotal C1-P1 bond so that the sum of the C1-P1 and P1-O2 bond lengths remains virtually constant.

The shortening of the P-O2 bond distance, which can be attributed to resonance stabilization of the negative charge by delocalization over the O1-P-O2 moiety, is well reproduced by DFT computations (Table 2). The Mayer bond indices (MBIs) calculated for ferrocenylphosphonic acid and the corresponding monoanion as model compounds at the M06/def-TZVP:sdd(Fe) level of theory support this explanation, revealing the significantly increased bond order of the P-O2 bond (1.863) and the slightly decreased bond order of the P-O1 bond (1.818). Consequently, P-O1 and P-O2 bonds have very similar lengths, shorter than the remaining P-OH bond. The calculated charges, which are very similar at the three oxygen atoms in $FcPO_3H_2$, somewhat differentiate upon deprotonation. The largest negative charge in $FcPO_3H^-$ is found at the O2 oxygen atom, as expected.

Table 2
Calculated bond distances, Mayer bond indices (MBIs) and Merz-Kollman charges (MKs) at the oxygen atoms.

Compound	Bond	Bond distance [Å]	MBIs	MKs
$FcPO_3H_2$	P-O1	1.462	1.961	−0.63
	P-O2	1.602	1.153	−0.62
	P-O3	1.590	1.169	−0.58
$FcPO_3H^-$	P-O1	1.481	1.818	−0.73
	P-O2	1.485	1.863	−0.79
	P-O3	1.649	0.982	−0.69

Salts **5** and **6** incorporated molecules of halogenated solvents, used during the crystallisation, in their structures. Unfortunately, the solvent molecules were severely disordered within the structural voids and had to be eliminated from the structure model (see Experimental). Notably, the crystal assembly of the ions that form the structure of salt **5** is relatively simple (Fig. 4), reflecting the prevalence of H-bond acceptors over conventional H-bond donors (OH, NH). Specifically, the anions H**L**$^-$ associate into dimers around crystallographic inversion centres through charge-supported O-H···O$^-$ hydrogen bonds (O2···O3 = 2.533(4) Å), while the phosphoryl oxygens O1 form additional hydrogen bonds with the NH groups of the adjacent cations $(dabcoH)^+$ (O1···N1 = 2.597(4) Å). Conversely, the supramolecular assembly of **6** is relatively complex due to the presence of additional H-bond donors in the structure (Fig. 5). Similarly to **5**, the phosphonate moieties form dimeric units *via* the O3-H···O2 interactions, whose midpoints coincide with the crystallographic inversion centres (O2···O3 = 2.554(1) Å). Furthermore, each phosphonate moiety acts as a hydrogen bond acceptor for a proximal ammonium cation, forming two O-H···O bonds (O4···O2 = 2.669(2) Å, O5···O1 = 2.696(1) Å) and one relatively longer N-H···O hydrogen bond (N2···O1 = 3.054(2) Å). The resulting $\{(HOCH_2CH_2)_2NH_2\}_2\{H\mathbf{L}\}_2$ motifs are interlinked into a two-dimensional array by additional N-H···O interactions towards the P=O oxygen (N···O1 = 2.853(2) Å) and by N-H···OH interactions (N···O4 = 2.902(2) Å).

2.2. Preparation and characterisation of Pd(II) complexes

A series of Pd(II) complexes [17] was prepared and structurally characterised to study the coordination behaviour of $H_2\mathbf{L}$. Various Pd(II) precursors were used in the testing reactions, differing in supporting ligands and in the number of accessible coordination sites at the central Pd(II) ion, including those that may possibly

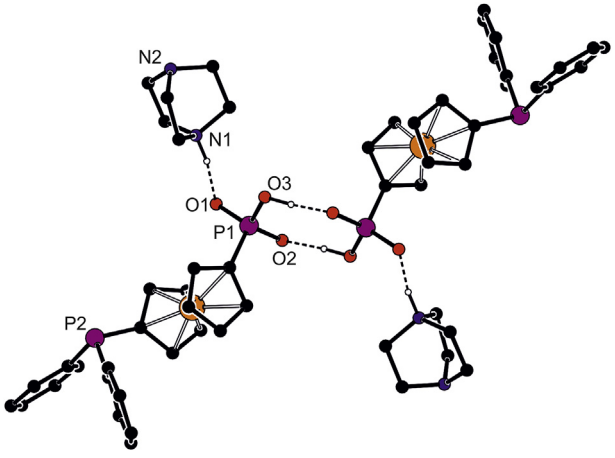

Fig. 4. Hydrogen-bonded dimers in the crystal structure of **5**; only NH hydrogens are shown for clarity.

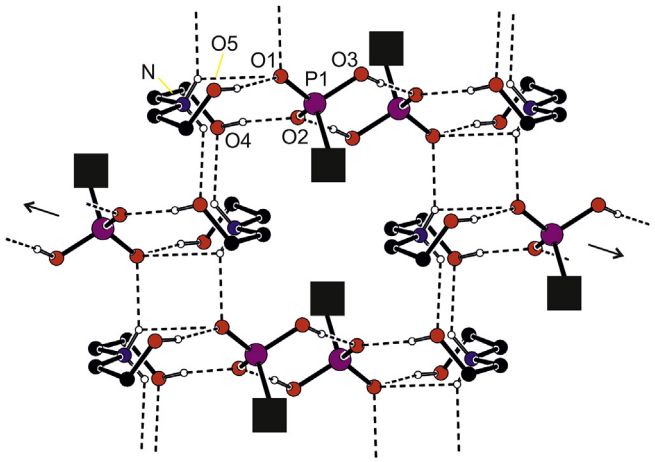

Fig. 5. Section of the hydrogen-bonded assembly in the crystal structure of **6**; for clarity, the bulky phosphinoferrocenyl moieties are replaced with black boxes, and only the NH and OH hydrogens are shown. The arrows indicate lateral propagation of the columnar arrays.

assist in the $H_2\mathbf{L}$ conversion into a phosphino-phosphonate anion. Thus, the reaction of $H_2\mathbf{L}$ with $[PdCl_2(cod)]$ (cod = cycloocta-1,5-diene) produced the bis(phosphine) complex **7** (Scheme 3). The compound is relatively unstable, readily decomposing in solution, which in turn complicates the characterisation of the compound and its purification. For instance, attempts to purify **7** by crystallization typically resulted in massive losses of the material.

The ^{1}H NMR spectra of **7** display broad signals due to the ferrocene and PPh_2 fragments at the expected positions, and the coordination of the phosphine moiety is manifested as a shift of the ^{31}P NMR resonance to a lower field (δ_P 17.0 ppm; N.B. the signals due to the phosphonate moiety is observed as a broad singlet at δ_P 18.0). Repeated attempts to obtain crystalline material suitable for X-ray diffraction analysis eventually afforded crystals of the stoichiometric solvate **7**·3EtOH from ethanol/diethyl ether (Fig. 6). The geometry of the coordination sphere around Pd(II) is similar to that of the formally parent compound *trans*-$[PdCl_2(FcPPh_2$-$\kappa P)_2]$ [6a], and the parameters of the independent but chemically equivalent halves of the complex molecule differ only marginally. The bulky phosphinoferrocene ligands occupy mutually opposite positions, highlighting the near centrosymmetric arrangement of the complex (accordingly, the phosphonate units are directed away from the ligated metal centre with τ(Fe1) and τ(Fe2) of −145.0(1)° and 139.7(1)°). In turn, this suggests that the relatively lower symmetry of the complex molecule results from intermolecular interactions and from the overall symmetry of the crystal array rather than from any intrinsic asymmetry (*e.g.*, in ligand coordination).

In the crystal, ferrocene ligands from different complex molecules pair into dimers through $(O\text{-}H\cdots O{=}P)_2$ interactions involving their uncoordinated phosphonate groups. These fragments further assemble into infinite chains *via* interactions between the remaining phosphonate OH moieties and the solvating ethanol

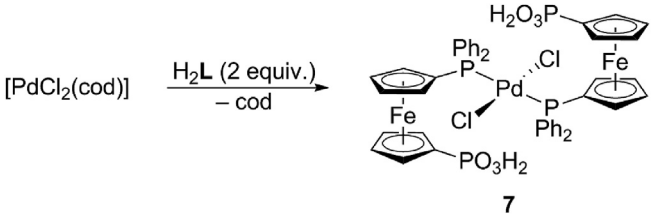

7

Scheme 3. Synthesis of the bis(phosphine) complex **7** (cod = cycloocta-1,5-diene).

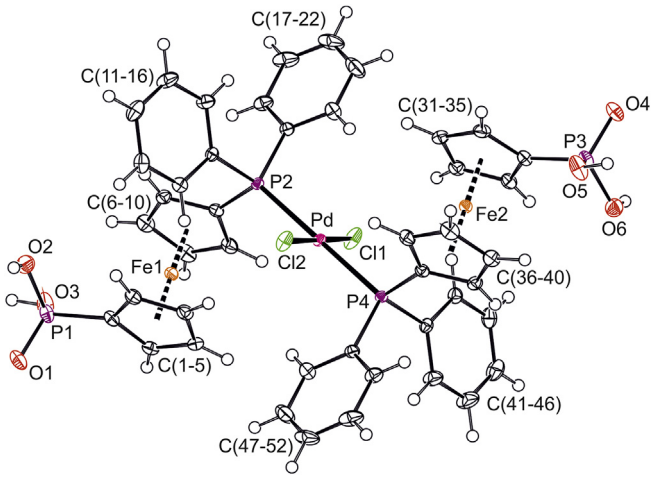

Fig. 6. View of the complex molecule in the structure of **7**·3EtOH. Displacement ellipsoids at the 50% probability level. Selected distances and angles (in Å and deg): Pd-Cl1 2.2989(5), Pd-Cl2 2.2980(5), Pd-P2 2.3440(4), Pd-P4 2.3328(4), Cl1-Pd-P2 88.04(2), Cl1-Pd-P4 92.19(2), Cl2-Pd-P2 92.90(2), Cl2-Pd-P4 86.87(2), P1-O1 1.502(1), P1-O2 1.556(1), P1-O3 1.547(1), P1-C1 1.768(2), P2-C6 1.802(1), P2-C11 1.830(1), P2-C17 1.818(1), P3-O4 1.501(1).

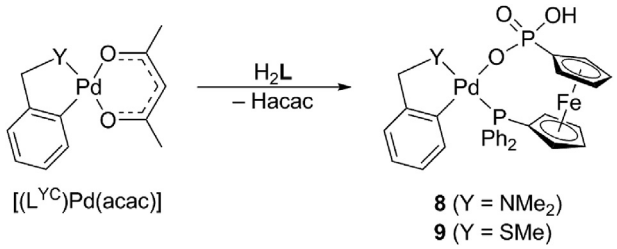

Scheme 4. Synthesis of Pd(II) complexes with supporting *ortho*-metallated ligands (Hacac = acetylacetone).

molecules (Fig. 7). The phosphoryl oxygen atoms (P=O) serve as additional H-bond acceptors for these interactions. When combined, hydrogen bond interactions give rise to layers oriented parallel to the crystallographic (1 1 1) planes.

When mixed with Pd(II) acetylacetonate (acac) complexes containing supporting o*rtho*-palladated ligands, *viz*. [(L^{CY})Pd(acac)], where L^{CY} = 2-[(dimethylamino-κ*N*)methyl]phenyl-κC^1 and 2-[(methylthio-κ*S*)methyl]phenyl-κC^1, H_2**L** produced the neutral bis-chelate complexes **8** and **9** (Scheme 4), formed through proton transfer from H_2**L** to the acetylacetonate ligand and through O,P-chelating coordination of the formed anion H**L**$^-$.

Compounds **8** and **9** result as yellow solids and are stable under ambient conditions. Their ^{1}H and ^{13}C NMR spectra display signals attributable to the ferrocene phosphino-phosphonate and to the respective *ortho*-metallated ligand. The resonances of the CH_2SMe/CH_2NMe_2 arms are split into ^{31}P-coupled doublets, thus suggesting a *trans*-P,N/S relationship for both compounds. The ^{31}P NMR signals attributable to the Pd-bound phosphine moieties are identified (in $CDCl_3$) as singlets at δ_P 29.1 and 26.2 ppm for **8** and **9**, respectively, whereas the resonances of the O-coordinated PO_3H^- units are found at δ_P 19.2 (**8**) and 19.9 ppm (**9**) (*i.e*., shifted to a higher field in relation to H_2**L** itself; δ_P 26.7 ppm in $CDCl_3$). ESI MS spectra further corroborate the formulation of **8** and **9**, showing $[M + H]^+$ ions.

Complexes **8** and **9** crystallise relatively willingly but tend to incorporate disordered solvent molecules in their crystals (see Experimental). In addition, compound **8** crystallizes with two structurally independent but otherwise very similar molecules in the asymmetric unit (space group *P*−1; for an overlap, see the Supporting Information, Figure S1). Views of the molecular structures of **8** (molecule 1) and **9** are presented in Fig. 8, and the relevant structural parameters are outlined in Table 3. The Pd-donor distances and the interligand angles determined for **8** and **9** are generally similar to those found in analogous complexes featuring O,P-chelating phosphinoferrocene sulfonate ligand $Ph_2PfcSO_3^-$ [6a]. Similarly to phosphino*sulfonate* complexes, the Pd-P bond length in **9** is significantly longer than in **8**, thus reflecting a stronger *trans* influence of the sulfur donor [18]. The coordination environments of the palladium(II) ions in **8** and **9** are distorted due to variations in individual Pd-donor distances and to steric demands of the chelate rings. However, the degree of distortion differs between the complexes. In **9**, which features the larger sulfur donor atom, the angle associated with the L^{CY} chelating ligand is larger (*i.e*., departs less from the ideal 90°) but the coordination plane is more severely twisted than in **8**, as shown by the dihedral angle of the {Pd,O,P} and {Pd,C,S} "half-planes" associated with the two chelate rings (16.09(7)°). The analogous angles subtended by the {Pd,O,P} and {Pd,C,N} planes in **8** are only 6.28(9)° (Pd1) and 8.60(9)° (Pd2).

O,P-chelating coordination requires that the donor moieties of the phosphinophosphonate anion H**L**$^-$ be rotated into positions closer than those found in the crystal structures discussed above (H_2**L**, its salts and complex **7**). Consequently, the conformations of the 1,1′-disubstituted ferrocene units in **8** and **9** are between synclinal staggered (ideal value: 36°) and synclinal eclipsed (ideal value: 72°), characterised by τ angles of 53.2(2)° (**8**, molecule 1), 42.9(2)° (**8**, molecule 2), and 39.6(1)° (**9**). In addition, the

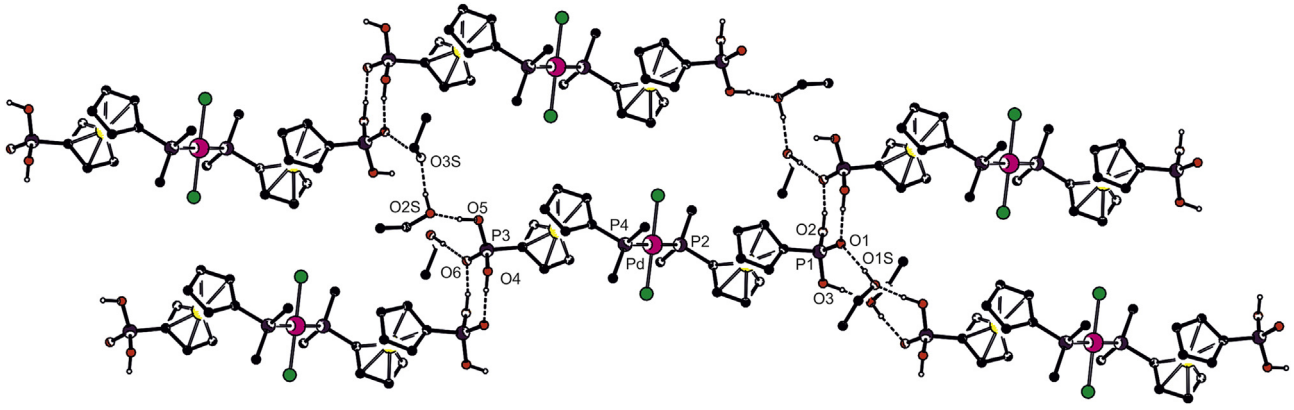

Fig. 7. Section of the hydrogen-bonded assembly in the structure of **7**·3EtOH. Only the OH hydrogens and the pivotal atoms from the phenyl rings are shown for clarity. Hydrogen bond parameters (in Å): O2···O4 2.559(2) Å, O3···O1S 2.502(2), O5···O2S 2.488(2), O6···O1 2.616(2), O1S···O1 2.669(2), O2S···O3S 2.622(2), O3S···O4 2.712(2).

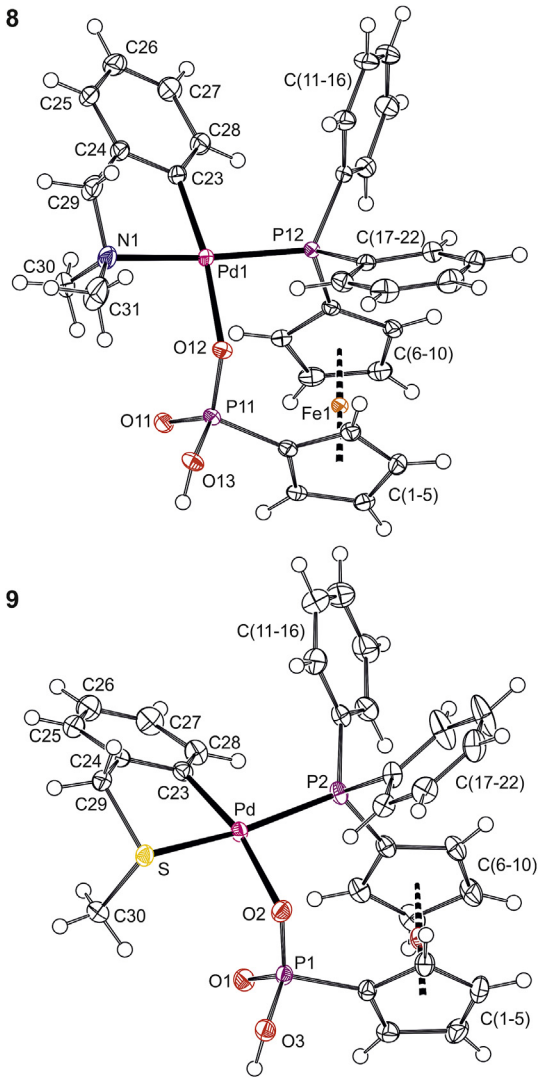

Fig. 8. PLATON plots of the molecular structures of **8** (molecule 1) and **9** (molecule 2); displacement ellipsoids at the 50% probability level.

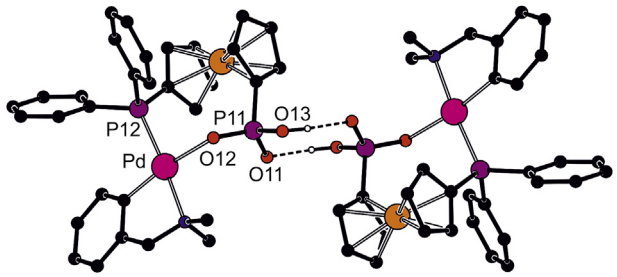

Fig. 9. Hydrogen-bonded dimeric motif in the structure of **8** (molecule 1 interacts with its inversion image); only OH hydrogens are shown for clarity.

deprotonation and coordination of the phosphonate group results in the differentiation of the P-O distances, as observed in salts **5** and **6**. In particular, the P=O and P-O(Pd) bonds of **8** and **9** are shorter than the P-OH bond involved in hydrogen bonding interactions.

In the crystals of **8** and **9**, the complex associates through pairs of O-H···O=P hydrogen bonds into dimers around the crystallographic inversion centres (in **8**, the dimers are formed between molecules 1 or 2 separately). The intermolecular O···O distances are

Table 3
Selected distances and angles for **8** and **9** (in Å and deg).

Parameter	8 (molecule 1, Z = N)	8 (molecule 2, Z = N)	9 (Z = S)
Pd-P	2.2644(6)	2.2494(6)	2.3126(6)
Pd-O	2.137(2)	2.132(2)	2.145(2)
Pd-C	2.001(2)	1.988(2)	2.007(2)
Pd-Z	2.142(2)	2.144(2)	2.3292(6)
P-Pd-O	90.68(4)	89.28(5)	93.34(4)
P-Pd-C	97.05(6)	96.88(7)	97.87(6)
Z-Pd-O	91.36(7)	92.86(7)	85.67(4)
Z-Pd-C	81.18(8)	81.25(8)	84.98(6)
P=O	1.506(2)	1.504(2)	1.504(2)
P-O(Pd)	1.510(2)	1.511(2)	1.512(2)
P-OH	1.579(2)	1.573(2)	1.579(2)

2.588(2) Å (O13···O11), 2.522(2) Å (O23···O21) for **8**, and 2.584(2) Å (O3 ···O1) for **9**. Notably, both the symmetry of the crystal lattice (space group $P2_1/c$) and even the particular supramolecular interactions indicate that complex **9**, which contains a stereogenic sulfur atom, is obtained in racemic form (Fig. 9).

3. Conclusion

1'-(Diphenylphosphino)ferrocene-1-phosphonic acid (H_2**L**), a new addition into the family of polar phosphinoferrocene ligands, can be prepared in a conventional manner from the corresponding phosphonate ester. Although the compound is relatively unstable and spontaneously decomposes upon storage, it can be converted into acidic ammonium salts containing the anion H**L**$^-$ and used to prepare transition metal complexes. While in its native form compound H_2**L** coordinates soft Pd(II) ions as a P-monodentate donor, deprotonation to H**L**$^-$ (*e.g.*, by proton transfer to a suitable Pd-bound ligand) opens a convenient access to O,P-chelated complexes. The phosphonate moieties in the free acid H_2**L**, its salts and even the Pd(II) complexes participate in intermolecular (or interionic) hydrogen-bonding interactions. In turn, these interactions give rise to discrete or polymeric solid-state assemblies, whose complexity changes with the number of the available hydrogen bond donors and acceptors. Overall, the coordination behaviour of H_2**L** resembles that of phosphinoferrocene sulfonate **A** rather than the behaviour of the analogous phosphinocarboxylic ligand Hdpf, except that anion H**L**$^-$ resulting by monodeprotonation of H_2**L** retains one of its OH groups and can thus enter into hydrogen bonding interactions as a H-bond donor.

4. Experimental

4.1. Materials and methods

All preparations were performed under an argon atmosphere using standard Schlenk techniques. Compounds **2** [8], **3** [19], [(L^{NC})Pd(acac)] [20], and [(L^{YC})Pd(acac)] [21] were prepared according to literature procedures. Other chemicals were purchased from commercial suppliers (Sigma-Aldrich, Alfa-Aesar) and used as received. Anhydrous dichloromethane and THF were obtained using a PureSolv MD5 solvent purification system (Innovative Technology, Inc., Amesbury, MA, USA). Solvents for chromatography and crystallisations were of reagent grade (Lach-Ner, Czech Republic) and used without any additional purification step.

^{1}H, ^{31}P{^{1}H}, and ^{13}C{^{1}H} NMR spectra were recorded at 25 °C with a Varian Unity Inova 400 spectrometer operating at 400, 101 and 162 MHz for ^{1}H, ^{13}C and ^{31}P, respectively. Chemical shifts (δ in ppm) are given relative to internal tetramethylsilane (^{1}H and ^{13}C) and to external 85% aqueous H_3PO_4 (^{31}P). In addition to the

standard notation of signal multiplicity (s = singlet, d = doublet, t = triplet, etc.) [22], vt and vq are used to distinguish virtual triplet and quartets arising from the second-order spin systems formed by cyclopentadienyl hydrogens. FTIR spectra were acquired on a Thermo Nicolet 6700 instrument over the 400–4000 cm^{-1} range. Electrospray ionization (ESI) mass spectra were recorded on a Compact QTOF-MS spectrometer (Bruker Daltonics) using samples dissolved in HPLC-grade methanol. Elemental analyses were performed with a PE 2400 Series II CHNS/O Elemental Analyser (Perkin Elmer). The amount of clathrated solvent (if present) was confirmed by NMR analysis.

4.2. Synthesis of [1'-(diphenylphosphino)ferrocenyl]phosphonic acid (H_2**L**)

Neat bromo-trimethylsilane (1.3 mL, 10 mmol) was added dropwise to a solution of ester **2** (1.67 g, 3.3 mmol) in dichloromethane (60 mL). The resulting mixture was stirred for 4 h and then evaporated under vacuum. The residue was dissolved in dichloromethane (10 mL) and treated with water (0.5 mL) under vigorous stirring for 30 min. The resulting mixture was dried over $MgSO_4$, filtered and evaporated under vacuum to afford an orange oily residue, which was purified by column chromatography over silica gel using chloroform-methanol (10:1) as eluent. A single orange band was collected and concentrated. The product was dissolved in chloroform (3 mL) and precipitated by adding an excess of hexane. The separated solid was filtered off, washed with hexane and dried under vacuum, yielding H_2**L**·0.5H_2O as a pale orange powder (1.02 g, 67%). Crystals of unsolvated H_2**L** suitable for X-ray diffraction analysis were obtained from ethyl acetate-hexane.

^{1}H NMR (dmso-d_6): δ 3.75 (very br s, 2 H, PO_3H_2), 4.02 (br s, 2 H, fc), 4.11 (br s, 2 H, fc), 4.24 (br s, 2 H, fc), 4.57 (br s, 2 H, fc) 7.25–7.38 (m, 10 H, PPh_2). ^{13}C{^{1}H} NMR (dmso-d_6): δ 71.13 (d, J_{PC} = 11 Hz, CH of fc), 71.50 (d, J_{PC} = 15 Hz, CH of fc), 73.25 (d, J_{PC} = 3 Hz, CH of fc), 73.44 (d, J_{PC} = 15 Hz, CH of fc), 75.80 (br d, J_{PC} = 6 Hz, *C*-PPh_2 of fc), 128.25 (d, J_{PC} = 7 Hz, CH of PPh_2), 128.55 (s, CH of PPh_2), 133.00 (d, J_{PC} = 20 Hz, CH of PPh_2), 138.73 (d, J_{PC} = 11 Hz, C_{ipso} of PPh_2). The signal due to ferrocene *C*–PO_3H_2 was not observed. ^{31}P{^{1}H} NMR (dmso-d_6): δ −17.4 (s, PPh_2), 17.3 (br s, PO_3H_2). ^{31}P{^{1}H} NMR ($CDCl_3$): δ −16.0 (s, PPh_2), 26.7 (br s, PO_3H_2). IR (Nujol): ν_{max} 1654 br m, 1586 m, 1437 m, 1309 m, 1195 s, 1161 m, 1122 w, 1070 w, 1034 s, 997s, 641 w, 573 s, 487 s, 455 m cm^{-1}. EI + MS: *m/z* 451 ($[M + H]^+$). Anal. Calc. for $C_{22}H_{20}O_3FeP_2$·0.5H_2O (459.2): C 57.54, H 4.61%. Found: C 57.60, H 4.55%.

4.3. Synthesis of diethyl [1'-(diphenylphosphino)ferrocenyl] phosphonate–borane (1/1) (**4**)

A stirring solution of 1-(diphenylphosphino)-1′-bromferrocene–borane (**3**; 1.85 g, 4.0 mmol) in dry THF (150 mL) was cooled in a dry ice/ethanol bath to −78 °C and treated with *n*-butyllithium (1.6 mL of 2.5 M in hexanes, 0.44 mmol). After stirring the reaction mixture for 15 min, neat diethyl chlorophosphate (0.8 mL, 0.55 mmol) was introduced, and the mixture was stirred at −78 °C for another 15 min and then at room temperature for 3 h. Then, it was evaporated under reduced pressure, and the residue was purified by column chromatography over alumina. Chloroform-diethyl ether (2:3) was used to remove non-polar byproducts (mostly $FcPPh_2$·BH_3). Subsequent elution with chloroform-diethyl ether (3:2) eluted ester **4**. Yield: 1.39 g (60%), an orange oil.

^{1}H NMR ($CDCl_3$): δ 1.20 (br s, 3 H, BH_3), 1.30 (t, $^3J_{HH}$ = 7.1 Hz, 6 H, CH_3), 4.06 (q, $^3J_{HH}$ = 7.0 Hz, 4 H, CH_2), 4.38 (br s, 4 H, fc), 4.52 (vq, J' = 1.7 Hz, 2 H, fc), 4.74 (vq, J' = 1.0 Hz, 2 H, fc), 7.39–7.44 (m, 4 H, PPh_2), 7.45–7.51 (m, 2 H, PPh_2), 7.54–7.61 (m, 4 H, PPh_2). ^{31}P{^{1}H} NMR ($CDCl_3$): δ 16.3 (br d, J_{PH} = 55 Hz, PPh_2BH_3), 24.8 (s, PO_3Et_2). ^{13}C{^{1}H}: δ 16.43 (d, $^3J_{PC}$ = 6 Hz, CH_3), 61.82 (d, $^2J_{PC}$ = 6 Hz, CH_2), 70.54 (d, J_{PC} = 67 Hz, *C*-PO_3Et_2), 72.78 (d, J_{PC} = 15 Hz, CH of fc), 73.84 (d, J_{PC} = 13 Hz, CH of fc), 74.05 (d, J_{PC} = 10 Hz, CH of fc), 74.74 (d, J_{PC} = 7 Hz, CH of fc), 128.50 (d, J_{PC} = 10 Hz, CH of PPh_2), 130.82 (d, $^1J_{PC}$ = 82 Hz, C_{ipso} of PPh_2), 131.04 (d, J_{PC} = 2 Hz, CH of PPh_2), 132.60 (d, J_{PC} = 9 Hz, CH of PPh_2). The signal due to ferrocene *C*-PPh_2 was not observed. IR (Nujol): ν_{max} 3460 br s, 3077 m, 3056 s, 2386 s, 2254 m, 1653 m, 1589 w, 1574 w, 1484 m, 1437 s, 1390 s, 1370 s, 1313 m, 1248 s, 1189 s, 1106 s, 1033 s, 962 s, 834 s, 795 m, 739 s, 700 s, 639 m, 623 m, 595 s, 527 s, 490 s cm^{-1}. ESI + MS: *m/z* 519 ($[M - H]^+$), 521 ($[M + H]^+$). Anal. Calc. for $C_{26}H_{31}BFeO_3P_2$·2/3CH_2Cl_2 (576.6): C 55.53, H 5.65%. Found: C 55.34, 5.55%.

4.4. Synthesis of [1'-(diphenylphosphino)ferrocenyl]phosphonic acid–borane (1/1) (H_2**L**·BH_3)

Bromo-trimethylsilane (1.1 mL, 8.0 mmol) was added dropwise to a solution of adduct **4** (1.39 g, 2.7 mmol) in dichloromethane (60 mL), and the mixture was stirred for 4 h before evaporation under vacuum. The residue was taken up with dichloromethane (10 mL), and the solution was treated with water (0.5 mL) under stirring for 30 min. The resulting mixture was dried over $MgSO_4$, filtered and evaporated under vacuum to give an orange oily residue, which was purified by column chromatography over silica gel using a dichloromethane-methanol (10:1) as eluent. A single orange band was collected and evaporated. The product was redissolved in chloroform (3 mL) and precipitated by adding an excess of hexane. The separated solid was filtered off, washed with hexane and dried under vacuum to give H_2**L**·BH_3 as an orange solid (0.91 g, 73%).

^{1}H NMR (dmso-d_6): δ 1.20 (very br s, 3 H, BH_3), 4.04 (vq, J' = 1.8 Hz, 2 H, fc), 4.20 (vq, J' = 2.2 Hz, 2 H, fc), 4.25 (very br s, 2 H, OH), 4.49 (vq, J' = 1.8 Hz, 2 H, fc), 4.72 (br d, J' = 1.4 Hz, 2 H, fc), 7.47–7.58 (m, 10 H, PPh_2). ^{13}C{^{1}H} NMR (dmso-d_6): δ 68.80 (d, J_{PC} = 68 Hz, *C*-PPh_2 of fc), 71.93 (d, J_{PC} = 15 Hz, CH of fc), 72.19 (d, J_{PC} = 13 Hz, CH of fc), 73.40 (d, J_{PC} = 10 Hz, CH of fc), 74.55 (d, J_{PC} = 8 Hz, CH of fc), 74.89 (d, J_{PC} = 202 Hz, *C*-PO_3H_2 of fc), 128.73 (d, J_{PC} = 10 Hz, CH of PPh_2), 130.64 (d, J_{PC} = 60 Hz, C_{ipso} of PPh_2), 131.21 (d, J_{PC} = 2 Hz, CH of PPh_2), 132.10 (d, J_{PC} = 10 Hz, CH of PPh_2). ^{31}P{^{1}H} NMR (dmso-d_6): δ 15.6 (br s, PPh_2), 17.8 (s, PO_3H_2). IR (Nujol): IR (Nujol): ν_{max} 2725 w, 2383 s, 1683 w, 1588 w, 1467 s, 1377 s, 1312 w, 1256 w, 1197 s, 1174 s, 1107 s, 1059 s, 1036 s, 999 s, 943 m, 886 m, 837 s, 739 s, 698 s, 639 m, 624 m, 610 w, 576 m, 527 m, 475 s cm^{-1}. ESI + MS: *m/z* 487 ($[M + H]^+$). Anal. Calc. for $C_{22}H_{23}BFeO_3P_2$ (464.0): C 56.94, H 5.00%. Found: C 56.65, H 5.08%.

4.5. Synthesis of [1'-(diphenylphosphinoyl)ferrocenyl]phosphonic acid (H_2**L**O)

Hydrogen peroxide in excess (0.2 mL, 30% in H_2O) was added dropwise to a solution of H_2L (90 mg, 0.20 mmol) in acetone (5 mL). The resulting mixture was stirred for 1 h, dried over $MgSO_4$, filtered and evaporated under vacuum. The product was dissolved in dichloromethane (3 ml) and precipitated by adding excess of hexane. The separated solid was filtered off, washed with hexane and dried under vacuum, yielding H_2LO·H_2O as an orange solid (50 mg, 52%).

^{1}H NMR (dmso-d_6): δ 4.24 (br s, 2 H, fc), 4.37 (br s, 2 H, fc), 4.51 (br s, 2 H, fc), 4.73 (br s, 2 H, fc), 7.53–7.73 (m, 10 H, P(O)Ph_2). ^{13}C{^{1}H} NMR (dmso-d_6): δ 71. 52 (d, J_{PC} = 13 Hz, CH of fc), 71.63 (d, J_{PC} = 115 Hz, *C*-PPh_2 of fc), 72.53 (d, J_{PC} = 15 Hz, CH of fc), 73.48 (d, J_{PC} = 6 Hz, CH of fc), 73.60 (d, J_{PC} = 9 Hz, CH of fc), 74.50 (d, J_{PC} = 198 Hz, C-PO_3H_2 of fc), 128.71 (d, J_{PC} = 12 Hz, CH of PPh_2), 130.77 (d, J_{PC} = 10 Hz, CH of PPh_2), 132.19 (d, J_{PC} = 3 Hz, CH of PPh_2), 132.58 (d, $^1J_{PC}$ = 107 Hz, C_{ipso} of PPh_2). ^{31}P {^{1}H} NMR (dmso-d_6):

δ 16.5 (s, PO_3H_2), 31.7 (s, P(O)Ph_2). IR (Nujol): ν_{max} 1706 m, 1591 w, 1310 w, 1152 s, 1122 s, 1098 m, 1072 m, 998 w, 941 w, 539 m, 752 m, 571 s, 534 m, 497 m cm^{-1}. ESI + MS: *m/z* 467 ($[M + H]^+$), 489 ($[M + Na]^+$). Anal. Calc. for $C_{22}H_{20}FeO_4P_2 \cdot H_2O$ (484.2): C 54.57, H 4.58%. Found: C 54.62, 4.17%.

4.6. Synthesis of (dabcoH)(H**L**) (**5**)

H_2**L** (67.5 mg, 0.15 mmol) and dabco (16.8 mg, 0.15 mmol) were dissolved in a mixture of dichloromethane (7 mL) and methanol (4 mL). After stirring for 30 min, the volatiles were removed under vacuum to produce salt **5** as an orange solid in quantitative yield (84.3 mg). The crystals used for structure determination were obtained by recrystallisation from chloroform/hexane.

^{1}H NMR ($CDCl_3$): δ 3.00 (s, 12 H, CH_2), 4.03 (s, 2 H, fc), 4.18 (s, 2 H, fc), 4.42 (s, 2 H, fc), 4.63 (s, 2 H, fc), 5.79 (very br s, 1 H, OH), 7.26–7.37 (m, 10 H, PPh_2). ^{13}C{^{1}H} NMR (dmso-d_6): δ 44.83 (s, CH_2 dabco), 70.54 (d, J_{PC} = 11 Hz, CH of fc), 71.56 (d, J_{PC} = 14 Hz, CH of fc), 73.27 (d, J_{PC} = 16 Hz, CH of fc), 73.35 (br s, CH of fc), 75.16 (d, J_{PC} = 7 Hz, *C*-PPh_2 of fc), 78.46 (d, J_{PC} = 199 Hz, *C*-PO_3H of fc), 128.19 (d, J_{PC} = 7 Hz, CH of PPh_2), 128.46 (s, CH of PPh_2), 132.99 (d, J_{PC} = 19 Hz, CH of PPh_2), 138.95 (d, J_{PC} = 11 Hz, C_{ipso} of PPh_2). ^{31}P{^{1}H} NMR (dmso-d_6): δ −17.1 (s, PPh_2), 14.8 (br s, PO_3H). ESI + MS: *m/z* 113 ($[C_6H_{13}N_2]^+$), 451 ($[H_2$**L** + H$]^+$). IR (Nujol): ν_{max} 3393 br m, 3051 w, 2725 w, 1981 w, 1697 w, 1585 w, 1568 w, 1541 w, 1318 m, 1230 m, 1208 w, 1192 w, 1181 m, 1139 s, 1060 s, 1027 m, 995 m, 972 m, 917 s, 881 s, 830 m, 784 w, 746 s, 698 s, 669 w, 650 w, 607 m, 583 s, 529 w, 502 s, 483 m, 457 m, 441 m, 423 w cm^{-1}. HR – MS: *m/z* 449 ($[PPh_2fcPO_3H]^-$). Anal. Calc. for $C_{28}H_{32}O_3N_2FeP_2 \cdot 0.5CH_2Cl_2$ (604.8): C 56.60, H 5.50, N 4.63%. Found: C 56.14, H 5.47, N 4.79%.

4.7. Synthesis of ((HOCH$_2$CH$_2$)$_2$NH$_2$)(H**L**) (**6**)

H_2**L** (90.0 mg, 0.20 mmol) and bis(2-hydroxyethyl)amine (21.0 mg, 0.20 mmol) were dissolved in acetone (5 mL), and the mixture was stirred for 15 min. Subsequent evaporation under vacuum left salt **6** as a yellow powder in quantitative yield (111 mg). Crystals suitable for X-ray diffraction analysis were obtained after layering the solution of the salt in dichloromethane-THF (1:1) with hexane.

^{1}H NMR (dmso-d_6): δ 2.91 (br s, 4 H, NCH_2), 3.64 (br s, 4 H, OCH_2), 3.93 (vq, J' = 1.8 Hz, 2 H, fc), 4.07 (vq, J' = 1.8 Hz, fc), 4.17 (vq, J' = 2.2 Hz, fc), 4.53 (vt, J' = 1.8 Hz, fc), 4.86 (very br s, 2 H, CH_2OH), 7.25–7.36 (m, 10 H, PPh_2). ^{13}C{^{1}H} NMR (dmso-d_6): δ 49.91 (s, NCH_2), 57.12 (s, OCH_2), 70.46 (d, J_{PC} = 12 Hz, CH of fc), 71.39 (d, J_{PC} = 14 Hz, CH of fc), 73.18 (d, J_{PC} = 15 Hz, CH of fc), 73.23 (d, J_{PC} = 5 Hz, CH of fc), 75.17 (d, J_{PC} = 7 Hz, *C*-PPh_2 of fc), 78.92 (d, J_{PC} = 195 Hz, *C*-PO_3H of fc), 128.20 (d, J_{PC} = 7 Hz, CH of PPh_2), 128.46 (s, CH of PPh_2), 132.99 (d, J_{PC} = 19 Hz, CH of PPh_2), 138.95 (d, J_{PC} = 11 Hz, C_{ipso} of PPh_2). ^{31}P{^{1}H} NMR (dmso): δ −17.1 (s, PPh_2), 15.0 (s, PO_3H). IR (Nujol): ν_{max} 2041 m, 1932 m, 1683 w, 1653 w, 1558 w, 1540 w, 1307 m, 1169 m, 1073 m, 1035 m, 971 m, 833 m, 695 m, 608 m, 569 m, 483 m cm^{-1}. ESI + MS: *m/z* 451 ($[H_2$**L** + H$]^+$). Anal. Calc. for $C_{26}H_{31}O_5NFeP_2$ (555.3): C 56.23, H 5.63, N 2.52%. Found: C 56.01, H 5.47, N 2.37%.

4.8. Synthesis of trans-[PdCl$_2$(H$_2$**L**-κP)$_2$] (**7**)

H_2**L** (90.0 mg, 0.20 mmol) and [$PdCl_2$(cod)] (28.5 mg, 0.10 mmol) were dissolved in dichloromethane (30 mL), and the resulting mixture was stirred for 1 h. Then, the solvent was evaporated under reduced pressure, the residue was dissolved in methanol-dichloromethane (1:1, 10 mL), and the solution was precipitated by adding an excess of pentane-diethyl ether (1:1, 40 mL). The separated solid was filtered off, washed with pentane and dried under vacuum, affording **7**·0.5CH_2Cl_2 as a brown powder (88 mg, 79%). The crystals of **7**·3EtOH used for structure determination were grown by liquid-phase diffusion of diethyl ether into an ethanolic solution of the complex.

^{1}H NMR (dmso-d_6): δ 4.11 (very br s, 4 H, OH), 4.55 (br s, 8 H, fc), 4.70 (br s, 4 H, fc), 4.75 (br s, 4 H, fc), 7.38–7.60 (m, 20 H, PPh_2). ^{31}P{^{1}H} NMR (dmso-d_6): δ 17.0 (s, PPh_2), 18.0 (br s, PO_3H_2). IR (Nujol): ν_{max} 2726 w, 1653 br w, 1481 w, 1437 s, 1196 s, 1166 s, 1099 s, 1061w, 1035 s, 1000 s, 932 s, 884 m, 872 w, 841 m, 814 w, 748 m, 708 w, 696 s, 669 w, 644 w, 627 w, 580 m, 541 m, 507 s, 465 m, 455 w cm^{-1}. EIS + MS: *m/z* 1049 ($[PdL_2Na_2 + H]^+$). Anal. Calc. for $C_{44}H_{40}O_6Cl_2Fe_2P_4Pd \cdot 0.5CH_2Cl_2$ (1120.2): C 47.71, H 3.69%. Found: C 47.73, H 3.72%.

4.9. Synthesis of [(L^{NC})Pd(H**L**-κ^2O,P)] (**8**)

H_2**L** (36.0 mg, 0.08 mmol) and [(L^{NC})Pd(acac)] (27.2 mg, 0.08 mmol) were dissolved in dichloromethane (5 mL), and the reaction mixture was stirred for 30 min. Subsequent solvent removal produced **8**·0.25CH_2Cl_2 as a yellow solid. Yield: 50.0 mg (88%). Crystals of **8**·2CH_2Cl_2 suitable for X-ray diffraction analysis were obtained from dichloromethane/ethyl acetate/hexane.

^{1}H NMR ($CDCl_3$): δ 2.88 (s, 6 H, NMe_2), 3.99 (br s, 2 H, NCH_2), 4.02 (br s, 2 H, fc), 4.25 (br s, 2 H, fc), 4.57 (br s, 2 H, fc), 4.74 (br s, 2 H, fc), 5.85 (t, J = 7.1 Hz, 1 H, C_6H_4), 6.17 (t, J = 7.3 Hz, 1 H, C_6H_4), 6.66 (t, J = 7.32 Hz, 1 H, C_6H_4), 6.84 (t, J = 7.2 Hz, 1 H, C_6H_4), 7.22–7.29 (m, 4 H, PPh_2), 7.30–7.37 (m, 2 H, PPh_2), 7.55–7.64 (m, 4 H, PPh_2). ^{13}C{^{1}H} NMR ($CDCl_3$): 50.03 (br s, NMe_2), 70.59 (br s, CH of fc), 71.76 (d, J_{PC} = 53 Hz, *C*-PPh_2 of fc), 72.44 (br s, NCH_2), 72.52 (s, CH of fc), 74.23 (br d, J = 13 Hz, CH of fc), 76.53 (br s, partly overlapping with the solvent signal, CH of fc), ≈77.5 (d, *C*-PO_3H of fc; overlapping with the solvent resonance), 122.06 (s, CH of C_6H_4), 123.27 (s, CH of C_6H_4), 124.50 (d, J_{PC} = 5 Hz, CH of C_6H_4), 127.88 (d, J_{PC} = 11 Hz, PPh_2), 130.12 (s, CH of PPh_2), 133.59 (d, J_{PC} = 52 Hz, C_{ipso} of PPh_2), 134.62 (d, J_{PC} = 12 Hz, CH of PPh_2), 137.37 (d, J_{PC} = 10 Hz, CH of C_6H_4), 146.21 (s, C_{ipso} of C_6H_4), 148.38 (s, C_{ipso} of C_6H_4). ^{31}P{^{1}H} NMR ($CDCl_3$): δ 19.2 (s, PO_3H), 29.1 (s, PPh_2). IR (Nujol): ν_{max} 1168 br m, 1073 m, 1032 m, 930 m, 887 m, 844 m, 743 m, 696 m, 584 m, 485 m cm^{-1}. ESI + MS: *m/z* 690 ($[M + H]^+$). Anal. Calcd. for $C_{31}H_{31}FeNO_3P_2Pd \cdot 0.25CH_2Cl_2$ (711.0): C 52.79, H 4.47, N 1.97%. Found: C 52.79, H 4.56, 1.99%.

4.10. Synthesis of [(L^{SC})Pd(H**L**-κ^2O,P)] (**9**)

H_2**L** (36.0 mg, 0.08 mmol) and [(L^{SC})Pd(acac)] (27.5 mg, 0.08 mmol) were dissolved in dichloromethane (5 mL), and the resulting mixture was stirred for 30 min. Subsequent solvent removal afforded analytically pure **9** as a yellow solid. Yield 47.7 mg (86%). Recrystallization from dichloromethane-hexane gave single-crystals suitable for X-ray diffraction analysis.

^{1}H NMR ($CDCl_3$): δ 2.64 (d, J_{PH} = 3.6 Hz, 3 H, SMe), 4.05 (br s, 4 H, SCH_2 and fc), 4.31 (br s, 2 H, fc), 4.60 (br s, 2 H, fc), 4.79 (br s, 2 H, fc), 6.11 (br m, 2 H, C_6H_4), 6.59 (br t, J = 7.5 Hz, 1 H, C_6H_4), 6.84 (br d, J = 7.5 Hz, 1 H, C_6H_4), 7.20–7.28 (m, 4 H, PPh_2), 7.29–7.35 (m, 2 H, PPh_2), 7.51–7.60 (m, 4 H, PPh_2). ^{13}C{^{1}H} NMR ($CDCl_3$): δ 20.41 (s, SMe), 46.23 (s, SCH_2), 70.61 (br s, CH of fc), 71.64 (d, J_{PC} = 51 Hz, *C*-PPh_2 of fc), 72.58 (d, J_{PC} = 8 Hz, CH of fc), 74.25 (d, J_{PC} = 13 Hz, CH of fc), 76.66 (d, overlapping with the solvent resonance, CH of fc), ≈78.5 (d, *C*-PO_3H of fc, partly overlapped by the solvent signal), 123.20 (s, CH of C_6H_4), 123.83 (s, CH of C_6H_4), 125.01 (d, J_{PC} = 6 Hz, CH of C_6H_4), 127.94 (d, J_{PC} = 11 Hz, CH of PPh_2), 130.15 (s, CH of PPh_2), 133.00 (d, J_{PC} = 50 Hz, C_{ipso} of PPh_2), 134.54 (d, J_{PC} = 12 Hz, CH of PPh_2), 139.46 (d, J_{PC} = 13 Hz, CH of C_6H_4), 147.26 (s, C_{ipso} of C_6H_4), 149.80 (s, C_{ipso} of C_6H_4). ^{31}P{^{1}H} NMR ($CDCl_3$): δ 19.9 (s, PO_3H), 26.2 (s, PPh_2). IR (Nujol): ν_{max} 3056 m, 1717 br m, 1573 m, 1483 m, 1436 s,

1312 m, 1260 m, 1196 s, 1166 m, 1148 s, 1095 m, 1068 s, 1046 w, 1029 m, 998 w, 971 w, 924 s, 889 m, 826 m, 751 m, 735 m, 694 s, 653 w, 626 w, 584 s, 539 m, 519 m, 482 s, 470 s, 449 w cm^{-1}. ESI + MS: *m/z* 693 ($[M + H]^+$). Anal. Calc. for $C_{30}H_{28}FeO_3P_2PdS$ (692.8): C 52.01, H 4.07%. Found: C 51.96, H 4.10%.

4.11. X-ray crystallography

Diffraction data ($\pm h \pm k \pm l$, $\theta_{max} = 27.5°$) were collected at 120(2) (for **5**) or 150(2) K (for all other compounds) using a Bruker D8 VENTURE Kappa Duo PHOTON100 instrument equipped with a IμS micro-focus X-ray tube (Mo Kα radiation, $\lambda = 0.71073$ Å). The structures were solved using direct methods (SHELXT [23]) and then refined using the full-matrix least-squares routine based on F^2 using SHELXL-2014 or SHELXL-2016 [24]. The non-hydrogen atoms were refined with anisotropic displacement parameters. The OH and NH hydrogens were identified on difference density maps and refined either freely (only for H_2**L**) or as riding atoms with U_{iso}(H) set to a 1.2U_{eq} of their bonding atom. Hydrogens at carbon atoms were included in their theoretical positions and refined analogously. In some cases, the analysed crystals contained disordered molecules of halogenated solvents used during the crystallisation (**5**: chloroform; **6**, **8** and **9**: dichloromethane). The contributions of these molecules to the overall scattering were numerically eliminated by PLATON SQUEEZE [25]. A recent version of the PLATON program [26] was used to perform all geometric calculations and to prepare the structural diagrams.

Selected crystallographic data, data collection and structure refinement parameters are available in Supporting Information. CCDC 1899917-1899922 contains supplementary crystallographic data on this paper. These data are available, free of charge from The Cambridge Crystallographic Data Centre via www.ccdc.cam.ac.uk/data_request/cif.

4.12. DFT computations

DFT calculations have been performed using the M06 density functional [27] and SDD (Fe) [28] and def2-TZVP (C, H, O and P) [29] basis sets together with Grimme's D3 dispersion correction [30], as implemented in the Gaussian 16 program package [31]. The solid-state structure of $FcPO_3H_2$ determined by X-ray diffraction analysis [13] was used as a starting point for geometry optimization. Mayer bond indices [32] and Merz-Kollman charges [33] were obtained using the software package Multiwfn [34].

Acknowledgements

This work was supported by the Charles University Research Centre program (project no. UNCE/SCI/014). Computational resources were provided by the CESNET (project LM2015042) and by the CERIT Scientific Cloud (project LM2015085), supported within the programme “Projects of Large Research, Development, and Innovations Infrastructures”.

Appendix A. Supplementary data

Supplementary data related to this article can be found at https://doi.org/10.1016/j.jorganchem.2019.04.012.

References

[1] a) N. Pinault, D.W. Bruce, Coord. Chem. Rev. 241 (2003) 1;
b) K.H. Shaughnessy, Chem. Rev. 109 (2009) 643;
c) F. Joó, Aqueous Organometallic Catalysis, Kluwer, Dordrecht, 2001;
d) B. Cornils, W.A. Herrmann (Eds.), Aqueous-Phase Organometallic Chemistry, second ed., Wiley-VCH, Weinheim, 2004.
[2] a) A. Bader, E. Lindner, Coord. Chem. Rev. 108 (1991) 27;
b) C.S. Slone, D.A. Weinberger, C.A. Mirkin, Prog. Inorg. Chem. 48 (1999) 233.
[3] a) Ferrocenes, in: A. Togni, T. Hayashi (Eds.), Homogeneous Catalysis, Organic Synthesis, Materials Science, VCH, Weinheim, 1995;
b) Ferrocenes, in: P. Štěpnička (Ed.), Ligands, Materials and Biomolecules, Wiley, Chichester, 2008;
c) R.C.J. Atkinson, V.C. Gibson, N.J. Long, Chem. Soc. Rev. 33 (2004) 313;
d) R. Gómez Arrayás, J. Adrio, J.C. Carretero, Angew. Chem. Int. Ed. 45 (2006) 7674.
[4] a) S.W. Chien, T.S.A. Hor, in: P. Štěpnička (Ed.), Ferrocenes: Ligands, Materials and Biomolecules, Wiley, Chichester, 2008, pp. 33–116, ch. 2;
b) K.-S. Gan, T.S.A. Hor, in: A. Togni, T. Hayashi (Eds.), Ferrocenes: Homogeneous Catalysis, Organic Synthesis, Materials Science, Wiley-VCH, Weinheim, 1995, pp. 3–104, ch. 1;
c) G. Bandoli, A. Dolmella, Coord. Chem. Rev. 209 (2000) 161.
[5] a) J. Podlaha, P. Štěpnička, J. Ludvík, I. Císařová, Organometallics 15 (1996) 543;
b) P. Štěpnička, Eur. J. Inorg. Chem. (2005) 3787.
[6] a) M. Zábranský, I. Císařová, P. Štěpnička, Organometallics 37 (2018) 1615;
b) M. Zábranský, I. Císařová, A.M. Trzeciak, W. Alsalahi, P. Štěpnička, Organometallics 38 (2019) 479.
[7] S. Basra, J.G. de Vries, D.J. Hyett, G. Harrison, K.M. Heslop, A.G. Orpen, P.G. Pringle, K. von der Luehe, Dalton Trans. (2004) 1901.
[8] P. Štěpnička, I. Císařová, R. Gyepes, Eur. J. Inorg. Chem. (2006) 926.
[9] a) T.L. Schull, J.C. Fettinger, D.A. Knight, Inorg. Chem. 35 (1996) 6717;
b) C.M. Reisinger, R.J. Nowack, D. Volkmer, B. Rieger, Dalton Trans. (2007) 272;
c) A. Labed, F. Jiang, I. Labed, A. Lator, M. Peters, M. Achard, A. Kabouche, Z. Kabouche, G.V.M. Sharma, C. Bruneau, ChemCatChem 7 (2015) 1090.
[10] a) O. Oms, F. Maurel, F.J. Le Bideau, A. Vioux, D. Leclercq, J. Organomet. Chem. 689 (2004) 2654;
b) C.E. McKenna, M.T. Higa, N.H. Cheung, M.-C. McKenna, Tetrahedron Lett. (1977) 155.
[11] L.D. Freedman, G.O. Doak, Chem. Rev. 57 (1957) 479.
[12] S.R. Alley, W. Henderson, J. Organomet. Chem. 637–639 (2001) 216.
[13] B.-Z. Yang, C. Xu, T.-K. Duan, W. Chen, Q.-F. Zhang, Acta Crystallogr. E: Struct. Rep. Online 67 (2011) m1087.
[14] J.A. Adeleke, L.-K. Liu, Acta Crystallogr. C: Struct. Chem. 49 (1993) 680.
[15] T.J.R. Weakley, Acta Crystallogr. Sect. B Struct. Crystallogr. Cryst. Chem. 32 (1976) 2889;
b) A.H. Mahmoudkhani, V. Langer, J. Mol. Struct. 609 (2002) 97.
[16] a) G. Ferguson, C. Glidewell, R.M. Gregson, P.R. Meehan, Acta Crystallogr. Sect. B Struct. Sci. 51 (1998) 129;
b) J. Beckmann, D. Dakternieks, A. Duthie, Appl. Organomet. Chem. 17 (2003) 817;
c) T. Diop, L. Diop, T. Maris, H. Stoeckli-Evans, Acta Crystallogr. E: Struct. Rep. Online 68 (2012) o1432;
d) M. Sarr, M.S. Boye, A. Diasse-Sarr, A. Grosjean, P. Guionneau, Acta Crystallogr. E: Struct. Rep. Online 68 (2012) o3087.
[17] C.F.J. Barnard, M.H.J. Russel, in: G. Wilkinson, R.D. Gillard, J.A. McCleverty (Eds.), Comprehensive Coordination Chemistry 5, Pergamon Press, Oxford, 1987, pp. 1099–1130;
b) A.T. Hutton, C.P. Morley, in: G. Wilkinson, R.D. Gillard, J.A. McCleverty (Eds.), Comprehensive Coordination Chemistry 5, Pergamon Press, Oxford, 1987, pp. 1157–1170;
c) F.R. Hartley, The Chemistry of Platinum and Palladium, Applied Science, London, 1973.
[18] a) T.G. Appleton, H.C. Clark, L.E. Manzer, Coord. Chem. Rev. 10 (1973) 335;
b) F.R. Hartley, Chem. Soc. Rev. 2 (1973) 163.
[19] K. Škoch, I. Císařová, J. Schulz, U. Siemeling, P. Štěpnička, Dalton Trans. 46 (2017) 10339.
[20] R. Navarro, J. García, E.P. Urriolabeitia, C. Cativiela, M.D. Diaz-de-Villegas, J. Organomet. Chem. 490 (1995) 35.
[21] M. Zábranský, I. Císařová, P. Štěpnička, Eur. J. Inorg. Chem. (2017) 2557.
[22] R.M. Silverstein, F.X. Webster, D.J. Kiemle, Spectrometric Identification of Organic Compounds, seventh ed., Wiley, Hoboken, 2005.
[23] G.M. Sheldrick, Acta Crystallogr. A: Found. Adv. 71 (2015) 3.
[24] G.M. Sheldrick, Acta Crystallogr., Sect. C, Struct. Chem. 71 (2015) 3.
[25] A.L. Spek, Acta Crystallogr. C: Struct. Chem. 71 (2015) 9.
[26] A.L. Spek, J. Appl. Crystallogr. 36 (2003) 7.
[27] Y. Zhao, D.G. Truhlar, Theor. Chem. Acc. 120 (2008) 215.
[28] D. Andrae, U. Haeussermann, M. Dolg, H. Stoll, H. Preuss, Theor. Chim. Acta 7 (1990) 123.
[29] F. Weigend, R. Ahlrichs, Phys. Chem. Chem. Phys. 7 (2005) 3297.
[30] a) S. Grimme, J. Antony, S. Ehrlich, H. Krieg, J. Chem. Phys. 132 (2010) 154104;
b) S. Grimme, S. Ehrlich, L. Goerigk, J. Comput. Chem. 32 (2011) 1456.
[31] Gaussian 16, Revision A. 03, M.J. Frisch, G.W. Trucks, H.B. Schlegel, G.E. Scuseria, M.A. Robb, J.R. Cheeseman, G. Scalmani, V. Barone, G.A. Petersson, H. Nakatsuji, X. Li, M. Caricato, A.V. Marenich, J. Bloino, B.G. Janesko, R. Gomperts, B. Mennucci, H.P. Hratchian, J.V. Ortiz, A.F. Izmaylov, J.L. Sonnenberg, D. Williams-Young, F. Ding, F. Lipparini, F. Egidi, J. Goings, B. Peng, A. Petrone, T. Henderson, D. Ranasinghe,

V.G. Zakrzewski, J. Gao, N. Rega, G. Zheng, W. Liang, M. Hada, M. Ehara, K. Toyota, R. Fukuda, J. Hasegawa, M. Ishida, T. Nakajima, Y. Honda, O. Kitao, H. Nakai, T. Vreven, K. Throssell, J.A. Montgomery Jr., J.E. Peralta, F. Ogliaro, M.J. Bearpark, J.J. Heyd, E.N. Brothers, K.N. Kudin, V.N. Staroverov, T.A. Keith, R. Kobayashi, J. Normand, K. Raghavachari, A.P. Rendell, J.C. Burant, S.S. Iyengar, J. Tomasi, M. Cossi, J.M. Millam, M. Klene, C. Adamo, R. Cammi, J.W. Ochterski, R.L. Martin, K. Morokuma, O. Farkas, J.B. Foresman, D.J. Fox, Gaussian, Inc., Wallingford CT, 2016.

[32] a) I. Mayer, Chem. Phys. Lett. 97 (1983) 270;
(b) I. Mayer, Int. J. Quantum Chem. 26 (1984) 151.

[33] a) U.C. Sing, P.A. Kollman, J. Comput. Chem. 5 (1984) 129;
(b) B.H. Besler, K.M. Merz, P.A. Kollman, J. Comput. Chem. 11 (1990) 431.

[34] T. Lu, F. Chen, J. Comput. Chem. 33 (2012) 580.